HHS Public Access

Author manuscript

Gastroenterology. Author manuscript; available in PMC 2019 December 01.

Published in final edited form as:

Gastroenterology. 2018 December ; 155(6): 1971–1984.e4. doi:10.1053/j.gastro.2018.09.010.

Expression of STING Is Increased in Liver Tissues from Patients With NAFLD and Promotes Macrophage-mediated Hepatic Inflammation and Fibrosis in Mice

Xianjun Luo[#1], **Honggui Li**[#1], **Linqiang Ma**[#1,2,3], **Jing Zhou**[1], **Xin Guo**[1], **Shih-Lung Woo**[1], **Ya Pei**[1], **Linda R. Knight**[4], **Michael Deveau**[4], **Yanming Chen**[5], **Xiaoxian Qian**[6], **Xiaoqiu Xiao**[2], **Qifu Li**[3], **Xiangbai Chen**[7], **Yuqing Huo**[8], **Kelly McDaniel**[9,10], **Heather Francis**[9,10], **Shannon Glaser**[9,10], **Fanyin Meng**[9], **Gianfranco Alpini**[9,10,†], and **Chaodong Wu**[1,†]

[1]Department of Nutrition and Food Science, Texas A&M University, College Station, TX 77843, USA,

[2]Department of Endocrinology, Texas A&M University, College Station, TX 77843, USA

[3]Department of the Laboratory of Lipid & Glucose Metabolism, the First Affiliated Hospital of Chongqing Medical University, Chongqing 400016, China;

[4]Department of Radiation Oncology, Veterinary Medical Teaching Hospital, Texas A&M University, College Station, TX 77843, USA,

[5]Department of Endocrinology, the Third Affiliated Hospital of Sun Yat-sen University, Guangzhou, Guangdong 510630, China;

[6]Department of Cardiology, the Third Affiliated Hospital of Sun Yat-sen University, Guangzhou, Guangdong 510630, China;

[7]Department of Pathology, Baylor Scott & White Health, College Station, TX 77845; USA

[8]Department of Vascular Biology Center, Department of Cellular Biology and Anatomy, Medical College of Georgia, Augusta University, Augusta, GA 30912, USA;

[9]Department of Research, Central Texas Veterans Health Care System

[†]Contact information Chaodong Wu, MD, PhD, College Station, TX 77843, cdwu@tamu.edu; or Gianfranco Alpini, PhD, Temple, TX 76504, galpini@tamu.edu.

AUTHOR CONTRIBUTION

X.L. carried out most of experiments involving mice. H.L. and L.M. carried out most of experiments involving cells. X.L., H.L., L.M., J. Z. X.G., S.L.W., Y.P. and K.M. collected tissue and cell samples and performed molecular and biochemical assays. H.L. performed histological and immunohistochemical assays. L.R.K. and M.D. performed mouse radiation. X.C. performed histology analysis of human liver sections. G.A. and C.W. came up the concept of the study. Y.C. X.Q., X.X., Q.L., Y.H., H.F., S.G., F.M., and G.A. contributed to scientific discussion. C.W. supervised all experiments and wrote the manuscript.

CONFLICT OF INTEREST

This material, in part, is the result of work supported with resources and the use of facilities at the Central Texas Veterans Health Care System, Temple, Texas. The content is the responsibility of the author(s) alone and does not necessarily reflect the views or policies of the Department of Veterans Affairs or the United States Government.

The authors have nothing to declare.

Author names in bold designate shared co-first authorship.

[10]Department of Medical Physiology, Texas A&M University College of Medicine, Temple, TX 76504

[#] These authors contributed equally to this work.

Abstract

Background & Aims: Transmembrane protein 173 (TMEM173 or STING) signaling by macrophage activates the type I interferon-mediated innate immune response. The innate immune response contributes to hepatic steatosis and non-alcoholic fatty liver disease (NAFLD). We investigated wither STING regulates diet-induced in hepatic steatosis, inflammation, and liver fibrosis in mice.

Methods: Mice with disruption of *Tmem173* (STING^{gt}) on a C57BL/6J background, mice without disruption of this gene (controls), and mice with disruption of *Tmem173* only in myeloid cells were fed a standard chow diet, a high-fat diet (HFD, 60% fat calories), or a methionine- and choline-deficient diet (MCD). Liver tissues were collected and analyzed by histology and immunohistochemistry. Bone marrow cells were isolated from mice, differentiated into macrophages, and incubated with DMXAA (an activator of STING) or cGAMP. Macrophages or their media were applied to mouse hepatocytes or human hepatic stellate cells (LX2) cells, which were analyzed for cytokine expression, protein phosphorylation, and fat deposition (oil red O staining following incubation with palmitate). We obtained liver tissues from patients with and without NAFLD and analyzed these by immunohistochemistry.

Results: Non-parenchymal cells of liver tissues from patients with NAFLD had higher levels of STING than liver tissues from patients without NAFLD. STING^{gt} mice and mice with disruption only in myeloid cells developed less severe hepatic steatosis, inflammation, and/or fibrosis following a HFD or MCD than control mice. Levels of phosphorylated JNK and p65 and the mRNAs encoding TNF, IL1B, and IL6 (markers of inflammation) were significantly lower in liver tissues from STING^{gt} mice vs control mice after a HFD or MCD. Transplantation of bone marrow cells from control mice to STING^{gt} mice restored the severity of steatosis and inflammation following a HFD. Macrophages from control, but not STING^{gt} mice, increased markers of inflammation in response to lipopolysaccharide and cGAMP. Hepatocytes and stellate cells co-cultured with STING^{gt} macrophages in the presence of DMXAA, or incubated with the medium collected from these macrophages, had decreased fat deposition and markers of inflammation compared to hepatocytes incubated with control macrophages.

Conclusions: We found levels of STING to be increased in liver tissues from patients with NAFLD mice with HFD-induced steatosis. In mice, loss of STING from liver macrophages reduces the severity of fibrosis and the inflammatory response. STING might be a therapeutic target for NAFLD.

Graphical Abstract

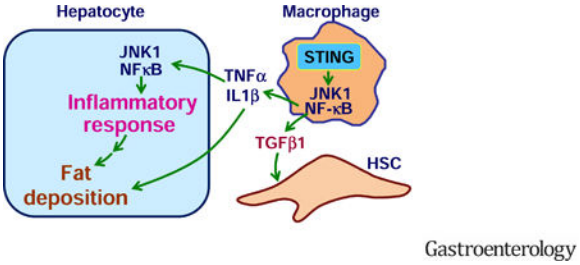

Keywords

IFN; HSC; NASH; LPS

INTRODUCTION

Non-alcoholic fatty liver disease (NAFLD) is characterized by hepatic steatosis [1, 2]. Simple steatosis may be benign, but progresses to non-alcoholic steatohepatitis (NASH) when the liver displays overt inflammatory damage [1, 2]. Epidemiological data indicate that NASH affects 1.5 to 6.45 percent of the general populations [3–5]. Alarmingly, the incidence of NASH in both adults and children is rising continuously due to ongoing epidemics of obesity [4, 5]. NASH is one of the most common causes of liver cirrhosis and hepatocellular carcinoma, ultimately leading to liver failure [6–9]. To date, there is no effective treatment for NASH [2, 10, 11].

Over the past decade, accumulating evidence validates an essential role for innate immunity in the development of hepatic steatosis and NASH [12–15]. As one of the most studied cell types in innate immunity, macrophages have drawn particular attention because macrophage proinflammatory activation is highly associated with hepatic steatosis and inflammation. When proinflammatory activation status increases, macrophages are capable of generating mediators that trigger or exacerbate hepatocyte inflammatory responses and fat metabolic dysregulation [14, 15]. To date, a number of regulators such as Jun-N terminal kinase 1 (JNK1), Period (Per)1/Per2, and adenosine 2A receptor are shown to alter the inflammatory status of macrophages, which in turn interact with hepatocytes to protect against or contribute to hepatic steatosis and inflammation [14–16]. These findings demonstrate the importance of the innate immune system, in particular macrophages, in pathophysiology of NAFLD. However, it remains largely unknown how regulators of innate immunity regulate hepatic metabolic, inflammatory, and fibrotic programs.

Transmembrane protein 173 (TMEM173) or stimulator of interferon genes (STING) is a signaling molecule whose activation elicits powerful type I interferon (IFN) immunity. Upon viral infection or endoplasmic reticulum (ER) stress, aberrant double-stranded DNA presents in cytosol and activates cyclic GMP-AMP (cGAMP) synthase (CGAS) to generate cGAMP. The latter activates STING and recruits STING to TANK-binding kinase 1 (TBK1), leading to activation of downstream signaling cascades involving interferon regulatory factor 3 (IRF3) to enhance transcriptions of type I IFN genes [20, 21]. This led to several recent studies to address how STING regulates liver injury induced by hepatitis B virus, carbon

tetrachloride (CCl_4), and/or nutrition stress [22–24]. Interestingly, the study by Thomsen et al. suggested that human and murine hepatocytes lack STING [22]. In contrast, several other studies suggest that mouse hepatocytes express STING, whose activation exerts a pro-apoptotic effect independent of inflammation [19, 25]. The study by Cho et al. also pointed to the importance of TBK1 activation, by cGAS-STING pathway and other unknown mediators, in the development of NASH. However, the relevance of STING to human NAFLD/NASH has not been reported. Also, STING activation by exogenous cGAMP reveals differential effects on the proinflammatory responses of macrophages and hepatocytes [26]. Given this, there is a critical need to elucidate the exact role for STING in the development and progression of NAFLD and liver fibrosis. The present study provides the primary evidence to support a deleterious role for STING in NAFLD and liver fibrosis, and this role of STING is likely mediated through enhancing macrophage proinflammatory activation.

MATERIALS AND METHODS

Animal experiments

Wild-type (WT) C57BL/6J and STING-disrupted ($STING^{gt}$) mice (C57BL/6J background) were obtained from Jackson Laboratory (Bar Harbor, ME). Chimeric mice in which STING was disrupted or intact only in myeloid cells were generated using bone marrow transplantation as described [14]. Mice were maintained on 12:12-h light-dark cycles (lights on at 06:00) and fed standard chow-diet (CD), high-fat diet (HFD, 60% fat calories), low-fat diet (LFD, 10% fat calories), and/or methionine- and choline-deficient diet (MCD) as detailed in Supplementary Information (SI). All diets are products of Research Diets, Inc (New Brunswick, NJ). All study protocols were reviewed and approved by the Institutional Animal Care and Use Committee of Texas A&M University.

Human liver samples

Liver sections of human subjects were generated from donated tissues by Sekisui-XenoTech, LLC (Kansas City, KS, USA). Subjects with NAFLD revealed severe hepatic steatosis compared with subjects without NAFLD (44.7 ± 10.6% fat content vs. 1.7 ± 1.9 %, assessed by Sekisui-XenoTech and by a board-certified pathologist (Dr. Xiangbai Chen, Baylor Scott & White Health, College Station, TX 77845)). Because of using fixed human tissues that are commercially available, the current study was exempted from the Institutional Review Board (IRB) approval.

Cell culture and treatment

Bone marrow cells were isolated from $STING^{gt}$ and WT mice and differentiated into macrophages (BMDM) [14]. After differentiation, $STING^{gt}$ and WT BMDM were treated with 5,6-dimethylxanthenone-4-acetic acid (DMXAA, an STING activator) (75 μg/mL) [27] or cGAMP (20 μg/mL) [26] and subjected to collection of conditioned media and examination of IFNβ production and the proinflammatory activation [26]. Some BMDM were trypsinized and added to primary mouse hepatocytes or LX2 cells (a cell line of human hepatic stellate cells, HSCs) at a 1:10 ratio for co-culture studies [15]. Hepatocytes or LX2 cells were incubated with BMDM-conditioned media and assayed for hepatocyte fat deposition and inflammatory

responses or HSC activation status. To examine the direct effect of STING on HSC activation, some LX2 were treated with DMXAA (75 μg/mL) in the absence or presence of transforming growth factor β1 (TGFβ1) (8 ng/mL for 24hr or 2.5 ng/mL for 48hr). Details were provided in SI.

Histological, biochemical and molecular assays

Liver sections were used for histological and immunohistochemical assays. Plasma parameters were measured using metabolic assay kits and ELISA kits. Also, tissue and/or cell samples were prepared for selected assays including Western blots analysis, real-time PCR, and other assays detailed in SI.

Statistical Methods

Numeric data are presented as means ± SD (standard deviation). Statistical significance was determined using unpaired, two-tailed ANOVA or Student's *t* tests. Differences were considered significant at the two-tailed $P < 0.05$.

RESULTS

NAFLD is coupled with increased liver signaling events downstream of STING

Activating STING recruits STING to TBK1 and activates TBK1 and IRF3 [19, 28, 29]. We analyzed the phosphorylation states of TBK1 and IRF3 in livers of WT C57BL/6J mice fed an HFD for 12 weeks. Upon HFD feeding, WT mice displayed obesity-associated NAFLD (Figure S1A-D). Additionally, the phosphorylation states of TBK1 and IRF3 in livers of HFD-fed WT mice were significantly higher than their respective levels in livers of LFD-fed mice (Figure S1E). These results validate that NAFLD is coupled with increased liver signaling events downstream of STING, and confirm that nutrition stress activates liver STING signaling pathway [26].

STING expression is increased in livers of human subjects with NAFLD

To address the relevance of STING to human NAFLD, we examined STING expression in liver sections of human subjects. Compared with control, liver sections of NAFLD patients revealed increased fat and collagen deposition indicated by H&E and Trichrome staining, respectively (Figure 1A, B), confirming hepatic steatosis and fibrosis. When STING expression was examined, the intensity of staining in liver sections of NAFLD patients was much stronger than that in subjects without NAFLD (Figure 1A, C). Also, most STING-positive cells in liver sections of NAFLD patients were aggregated relative to those in control. Further analysis by Dr. X. Chen indicated that STING-positive cells were mainly immune cells including macrophages/Kupffer cells and endothelial cells (Figure 1A). However, human liver sections did not reveal STING-positive hepatocytes. These results suggest that, in humans, STING is expressed in non-parenchymal liver cells, mainly macrophage/Kupffer cells. Moreover, STING expression is increased in livers of human patients with NAFLD.

STING disruption protects against HFD-induced NAFLD

We explored a role for STING in NAFLD using STING^{gt} and WT C57BL/6J mice. Under LFD-fed conditions, STING^{gt} mice did not differ significantly from WT mice in most parameters related to NAFLD and system metabolic homeostasis (Figure 2A-D; Figure S2). Upon HFD feeding for 12 weeks, WT mice, but not STING^{gt} mice, revealed overt NAFLD aspects. Specifically, STING^{gt} mice displayed a smaller gain in body weight compared with WT mice (Figure S2A). Body composition analysis indicated lower fat mass in HFD-STING^{gt} mice than in HFD-WT mice (Figure S2A); although the values of respiratory quotient (RQ) in HFD-STING^{gt} mice did not differ significantly from those in HFD-WT mice (Figure S2B). Also, HFD-STING^{gt} mice did not display systemic insulin resistance and glucose intolerance as did HFD-WT mice (Figure S2C, D). When NAFLD aspects were examined, plasma levels of alanine aminotransferase (ALT) in HFD-STING^{gt} mice were lower than those in HFD-WT mice (Figure 2A). Also, HFD-STING^{gt} mice displayed significant decreases in liver weight and hepatic levels of triglycerides compared with HFD-WT mice (Figure 2B, C). Consistently, HFD-STING^{gt} mice did not develop hepatic steatosis as did HFD-WT mice, indicated by H&E and/or oil red O staining of liver sections (Figure 2D; Figure S2E). When liver inflammatory status was examined, liver sections of HFD-STING^{gt} mice contained fewer F4/80-postivie cells (macrophages/Kupffer cells) compared with those of HFD-WT mice (Figure 2D). Moreover, the phosphorylation states of JNK p46 and NF0κB p65 and the mRNA levels of tumor necrosis factor alpha (TNFα), interleukin (IL)-1β, and IL-6 in livers of HFD-STING^{gt} mice were significantly lower than their respective levels in livers of HFD-WT mice (Figure 2E, F). With regard to fat metabolic genes/enzymes, liver mRNA levels of lipogenic enzymes such as acetyl-CoA carboxylase 1 (ACC1) and fatty acid synthase (FAS) in HFD-STING^{gt} mice also were significantly lower than their respective levels in HFD-WT mice (Figure 2F). These results, together with those presented in Figure 1, suggest that STING plays a detrimental role in NAFLD.

Myeloid cell-specific STING disruption decreases the severity of HFD-induced NAFLD

We sought to explore a role for the STING in macrophages in NAFLD using bone marrow transplantation (BMT), an approach that has been commonly used for altering macrophage gene expression [14, 30]. We transplanted bone marrow cells of STING^{gt} mice and/or WT mice to lethally irradiated WT mice. Upon HFD feeding for 12 weeks, WT/BMT-STING^{gt} mice, in which STING was disrupted only in myeloid cells, and WT/BMT-WT, in which STING was intact in all cells, gained similar body weight and revealed similar body composition (Figure S3A, B). However, HFD-fed WT/BMT-STING^{gt} mice displayed decreased severity of insulin resistance and glucose intolerance compared with HFD-fed WT/BMT-WT mice (Figure S3C, D). When NAFLD aspects were analyzed, HFD-fed WT/BMT-STING^{gt} mice showed decreased levels of plasma ALT and hepatic triglycerides compared with HFD-fed WT/BMT-WT mice; although the mice displayed comparable liver weight (Figure 3A-C). Additionally, HFD-fed WT/BMT-STING^{gt} mice revealed decreased severity of hepatic steatosis compared with HFD-fed WT/BMT-WT mice, indicated by H&E staining of liver sections (Figure 3D). When liver inflammatory status was examined, liver sections of HFD-fed WT/BMT-STING^{gt} mice contained fewer F4/80-positive cells than those of HFD-fed WT/BMT-WT mice (Figure 3D). FD-fed WT/BMT-STING^{gt} mice also revealed significant decreases in the phosphorylation states of JNK p46 and NFκB p65 and the mRNA levels of

TNFα, IL-1β, and IL-6 compared with HFD-fed WT/BMT-WT mice (Figure 3E, F). Relative to those in HFD-fed WT/BMT-WT mice, liver mRNA levels of FAS in HFD-fed WT/BMT-STING^{gt} mice were significantly decreased (Figure 3F); although liver mRNA levels of ACC1, CPT1a, and sterol regulatory element-binding protein 1c (SREBP1c) were not significantly altered. These results suggest that STING disruption specifically in myeloid cells (macrophages) decreases the severity of HFD-induced NAFLD.

STING presence specifically in myeloid cells exacerbates HFD-induced NAFLD

To further validate a role for the STING in macrophages in regulating the pathogenesis of NAFLD, we transplanted bone marrow cells of WT and/or STING^{gt} mice to lethally irradiated STING^{gt} mice. Upon HFD feeding, STING^{gt}/BMT-WT, in which STING was intact only in myeloid cells, and STING^{gt}/BMT-STING^{gt} mice, in which STING was disrupted in all cells, gained similar body weight and revealed similar body composition (Figure S4A, B). However, HFD-fed STING^{gt}/BMT-WT mice displayed increased severity of insulin resistance and glucose intolerance compared with HFD-fed STING^{gt}/BMT-STING^{gt} mice (Figure S4C, D). When NAFLD aspects were examined, HFD-fed STING^{gt}/BMT-WT mice revealed a significant increase in hepatic levels of triglycerides compared with HFD-fed STING^{gt}/BMT-STING^{gt} mice; although HFD-fed STING^{gt}/BMT-WT mice showed insignificant increases in plasma levels of ALT and liver weight (Figure 4A-C). Indicated by H&E staining of liver sections, HFD-fed STING^{gt}/BMT-WT mice revealed increased severity of hepatic steatosis compared with HFD-fed STING^{gt}/BMT-STING^{gt} mice (Figure 4D). Also, liver sections of HFD-fed STING^{gt}/BMT-WT mice contained significantly more F4/80-positive cells compared with those of HFD-fed STING^{gt}/BMT-STING^{gt} mice (Figure 4D). Consistently, livers of HFD-fed STING^{gt}/BMT-WT mice revealed significant increases in the phosphorylation states of JNK p46 and NFκB p65 and the mRNA levels of TNFα and IL-1β compared with those of HFD-fed STING^{gt}/BMT-STING^{gt} mice (Figure 4E, F). Relative to those in HFD-fed STING^{gt}/BMT-STING^{gt} mice, liver mRNA levels of FAS in HFD-fed STING^{gt}/BMT-WT mice were significantly increased (Figure 4F); although liver mRNA levels of ACC1, CPT1a, and SREBP1c were not significantly altered. These results suggest that STING presented only in myeloid cells (macrophages) triggers or exacerbates HFD-induced NAFLD. In combination, the results in Figures 3 and 4 strongly demonstrated a deleterious role for the STING in macrophages in the pathogenesis of NAFLD.

STING-driven macrophage factors enhance hepatocyte fat deposition and proinflammatory responses

To recapitulate our *in vivo* findings and gain mechanistic insights, we sought to validate STING regulation of macrophage activation and examine whether and how macrophage factors generated in response to STING activation or disruption regulate hepatocyte responses. In WT BMDM, cGAMP treatment caused a significant increase in LPS-induced phosphorylation states of JNK p46 (Figure S5A), confirming our previous finding [26]. Strikingly, in STING^{gt} BMDM, cGAMP treatment caused significant decreases in LPS-induced phosphorylation states of JNK p46 and in the mRNA levels of TNFα, IL-1β, and/or IL-6 under both basal and LPS-stimulated conditions (Figure S5B, C), indicating an essential role for STING in regulating macrophage activation. Next, we treated BMDM with

DMXAA to activate STING [27]. As expected, WT BMDM, but not STING^{gt} BMDM, revealed significantly increased production of IFNβ and phosphorylation states of JNK p46 and NFκB p65 (Figure 5A, B), validating that STING activation enhances proinflammatory responses of WT macrophages. These data are consistent with previous findings [31], which suggest that the proinflammatory effects of DMXAA are STING-dependent. Upon further analyses of macrophage polarization, we demonstrated that 15 STING disruption decreased macrophage proinflammatory activation, and exhibited marginal effects on macrophage alternative (M2) activation (Figure S6).

Next, we performed macrophage-hepatocyte co-cultures to examine whether STING facilitates macrophage generation of factors to promote NAFLD aspects. Palmitate-induced hepatocyte fat deposition in DMXAA-treated co-cultures of WT BMDM and hepatocytes was much greater than that in DMXAA-treated hepatocytes (without BMDM) (Figure 5C). This increase in hepatocyte fat deposition, however, was not observed in DMXAA-treated co-cultures of STING^{gt} BMDM and hepatocytes. We also incubated WT primary hepatocytes with macrophage-conditioned media (CM). When proinflammatory responses were analyzed, hepatocytes incubated with the CM of DMXAA-treated WT BMDM (DMX/WT BMDM-CM) displayed significant increases in LPS-stimulated phosphorylation states of JNK p46 and in the mRNA levels of TNFα, IL-1β, and/or IL-6 under both basal and LPS-stimulated conditions compared with hepatocytes incubated with the CM of control-treated WT BMDM (Ctrl/WT BMDM-CM) (Figure 5D, E). Of note, hepatocytes incubated with the CM of DMXAA-treated STING^{gt} BMDM (DMX/STING^{gt} BMDM-CM) revealed significantly decreased phosphorylation states of JNK p46 and NFκB p65 and mRNA levels of TNFα, IL-1β, and/or IL-6 under both basal and LPS-stimulated conditions compared with hepatocytes incubated with DMX/WT BMDM-CM (Figure 5D, E). With regard to the expression of fat metabolic genes/enzymes, hepatocytes incubated with DMX/WT BMDM-CM revealed significantly increased mRNA levels of ACC1, FAS, and SREBP1c compared with hepatocytes incubated with Ctrl/WT BMDM-CM (Figure 5F). These increases, however, were not observed in hepatocytes incubated with DMX/STING^{gt} BMDM-CM. Similar changes were observed in the mRNAs of TGFβ1 and fibronectin (Fn) (Figure 5F), which are mediators favoring liver fibrosis. Together, these results suggest that STING activation enables macrophages to generate factors that are capable of enhancing hepatocyte fat deposition and proinflammatory responses.

STING disruption decreases the severity of MCD-induced liver inflammation and fibrosis

NASH is the advanced form of NAFLD. We validated that liver TBK1 phosphorylation was increased in livers of MCD-fed mice (Figure S7). Next, we examined the effects of STING disruption on MCD-induced steatohepatitis and liver fibrosis. When fed a chow-diet, STING^{gt} mice did not differ significantly from WT mice in body weight, liver weight, and hepatic levels of triglycerides; although STING^{gt} mice revealed decreased phosphorylation states in liver JNK p46 and NFκB p65 (Figure S8). Upon MCD feeding, WT mice displayed overt hepatic steatosis and inflammation (Figures S7, S8). However, plasma levels of ALT, liver weight, and hepatic levels of triglycerides in MCD-STING^{gt} mice were significantly lower than their respective levels in MCD-WT mice (Figure 6A-C). Consistently, the severity of hepatic steatosis in MCD-STING^{gt} mice was significantly lighter than in MCD-

WT mice (Figure 6D). When stained for F4/80 expression, liver sections of MCD-WT mice revealed lots of F4/80-postivie cells, many of which were aggregated. However, liver sections of MCD-STING^{gt} mice contained significantly fewer aggregated F4/80-postivie cells (Figure 6D). Consistently, the phosphorylation states of JNK p46 and NFκB p65 and the mRNA levels of IL-1β in MCD-STING^{gt} mice were much lower than their respective levels in MCD-WT mice (Figure 6E, F). When liver fibrosis was ^{t} analyzed, liver sections of MCD-STING mice contained much lesser collagen compared with those of MCD-WT mice (Figure 6D). Also, hepatic protein content of α-smooth muscle actin significantly lower than their respective levels in MCD-WT mice (Figure 6E, F). These results suggest that STING disruption decreases the severity of MCD-induced NASH.

STING enhances the activation of hepatic stellate cells (HSCs)

To gain insights of STING regulation of NASH, we examined the direct effects of altering STING signaling on HSC activation. In LX2 cells, treatment with DMXAA in the presence of TGFβ1 significantly increased the phosphorylation states of p38 and protein amount of αSMA (Figure 7A, B). Additionally, DMXAA treatment significantly increased the mRNA levels of fibrogenic genes including Col1a1, αSMA, Fn, and TGFβ1 (Figure 7C). DMXAA treatment also caused an unexpected increase in PPARγ mRNAs, which may be a counter-regulatory response. In contrast, treatment with MRT67307, an inhibitor of TBK1, significantly decreased the effect of TGFβ1 on stimulating p38 phosphorylation (Figure S9). These results suggest a detrimental role for STING in promoting HSC activation.

Since NASH was characterized by massive macrophage aggregation (Figures S7B), we sought to examine whether STING-driven macrophage factors alter HSC activation. WT BMDM and STING^{gt} BMDM were pre-treated with DMXAA or control for 24 hr, trypsinized, and added to LX2 cells for 48 hr. In LX2 cells co-cultured with control-treated WT BMDM (Ctrl/WT BMDM), TGFβ1 treatment caused significant increases in p38 phosphorylation states and αSMA amount, indicating increased HSC activation. These effects of TGFβ1 were significantly enhanced in LX2 cells co-cultured with DMXAA-treated WT BMDM (DMX/WT BMDM), but not in LX2 cells co-cultured with DMXAA-treated STING^{gt} BMDM (DMX/STING^{gt} BMDM) (Figure 7D). Next, we incubated LX2 cells with macrophage-CM and examined HSC gene expression. The mRNA levels of Col1a1, Fn, and TGFβ1 in LX2 cells incubated with DMX/WT BMDM-CM were significantly higher than their respective levels in LX2 cells incubated with Ctrl/WT BMDM-CM (Figure 7E). However, the mRNA levels of Col1a1, Fn, and TGFβ1 in LX2 cells incubated with DMX/STING^{gt} BMDM-CM were lower than their respective levels in LX2 cells incubated with DMX/WT BMDM-CM, and comparable with their respective levels in LX2 cells incubated with Ctrl/WT BMDM-CM. Together, these results suggest that macrophage factors generated in response to STING activation enhance HSC activation.

DISCUSSION

STING is a powerful regulator of innate immunity [17, 20, 21]. In the present study, we validated in both animals and human subjects that liver STING is associated with hepatic steatosis and inflammation. Using various mouse models of NAFLD, we further validated

that STING plays a deleterious role in NAFLD. Notably, the STING found in myeloid cells (macrophages) is needed and sufficient for nutrition stress, e.g., HFD or MCD feeding, to trigger or exacerbate NAFLD/NASH aspects in mice. Mechanistically, STING activation markedly increases macrophage proinflammatory status, which in turn increases hepatocyte fat deposition and proinflammatory responses and enhances HSC activation. Therefore, we provided compelling evidence to demonstrate that STING plays a deleterious role in NAFLD through enhancing macrophage proinflammatory activation.

We have previously shown that HFD-fed WT mice display overt hepatic steatosis and inflammation compared with control mice [15]. In this model of NAFLD, we observed an increase n the phosphorylation states of liver TBK1 and IRF3, indicating increased signaling events downstream of STING. Similarly, we observed increased liver TBK1 phosphorylation in MCD-fed WT mice (a model of NASH), which was accompanied with increased liver proinflammatory status including massive macrophage aggregations. These results validated a link between STING signaling and NAFLD/NASH. Using liver sections of human subjects with NAFLD, we further validated the relevance of increased STING expression to human NAFLD. As such, we postulated a deleterious role for STING in NAFLD/NASH. In other words, we expected STING disruption to be protective and we found this to be true. In the present study, STING-disrupted mice were protected from HFD-induced NAFLD and revealed decreased severity of MCD-induced NASH compared with control mice. With regard to NAFLD/NASH pathogenesis, both hepatocytes and macrophages critically determine the development and progression of hepatic steatosis and inflammation [15, 16, 30, 32]. Considering this, STING found in either hepatocytes or macrophages could contribute to NAFLD/NASH. However, the study by Thomsen et al. indicated that human and murine hepatocytes are lack of STING [22]; although other studies suggest that mouse hepatocytes express STING [19, 23]. We confirmed that STING is not present in human hepatocytes, but expressed at high abundance in hepatic non-parenchymal cells. Because of this, to address a role for STING in macrophages is more relevant to human disease, e.g., NAFLD.

We provided two lines of evidence from chimeric mice to support a deleterious role for the STING in myeloid cells in the pathogenesis of NAFLD. In our loss-of-function study, chimeric mice whose STING was disrupted specifically in myeloid cells revealed decreased severity of HFD-induced hepatic steatosis and inflammation compared with mice whose STING was intact in all cells. In contrast, in our gain-of-function study, chimeric mice which had intact STING specifically in myeloid cells displayed increased severity of HFD-induced NAFLD aspects compared with chimeric mice whose STING was disrupted in all cells. These complementary results suggest that macrophage-specific STING is required, and is enough to generate factors that act on other liver cells, in particular hepatocytes, to promote hepatocyte fat deposition and enhance hepatocyte proinflammatory responses. Moreover, HFD-induced NAFLD aspects in chimeric mice whose STING was disrupted only in myeloid cells were similar to those in chimeric mice whose STING was disrupted in all cells whereas HFD-induced NAFLD aspects in chimeric mice whose STING was intact only in myeloid cells were similar to those in chimeric mice whose STING was intact in all cells. This implicates a greater contribution from macrophage-specific STING during NAFLD than from the STING found in other cells. As substantial evidence, treatment with

cGAMP or DMXAA significantly enhanced the effect of LPS on stimulating the proinflammatory activation of WT macrophages, but not STING^{gt} macrophages. More importantly, when co-cultured with primary mouse hepatocytes, DMXAA-treated WT macrophages, but not DMXAA-treated STING^{gt} macrophages, caused a significant increase in the degree of palmitate-induced hepatocyte fat deposition. Upon treating hepatocytes with macrophage-conditioned media, we also verified that STING-driven macrophage factors enhanced hepatocyte proinflammatory responses. In support of this, hepatocytes incubated with conditioned media of DMXAA-treated WT macrophages displayed significant increases in LPS-induced phosphorylation of JNK p46 and mRNA levels of TNFα, IL-1β, and IL-6 compared with hepatocytes incubated conditioned media of control-treated WT macrophages. These increases, however, were not observed in hepatocytes incubated with conditioned media of DMXAA-treated STING^{gt} macrophages, suggesting that STING disruption blunted the effect of DMXAA to drive macrophage production of factors that could enhance hepatocyte proinflammatory responses. Because of this, it is conceivable that STING-driven macrophage factors act to increase hepatocyte fat deposition and proinflammatory responses, thereby accounting for the development and progression of hepatic steatosis and inflammation.

Inflammation is key to drive NAFLD to NASH which is featured by inflammatory damage and liver fibrosis [16, 33]. In the present study, we also validated a deleterious role for STING in steatohepatitis and liver fibrosis. As supporting evidence, the levels of plasma ALT and hepatic triglycerides in MCD-STING^{gt} mice were significantly lower than their respective levels in MCD-WT mice. Additionally, the severity of liver proinflammatory responses, as well as liver deposition of collagen and amount/expression of αSMA, Col1a1, and Fn in MCD-STING^{gt} were much lower their respective levels in MCD-WT mice. These results are in agreement with the report that STING disruption protected mice from CCl_4-induced liver fibrosis [23]. The study by Iracheta-Vellve et al., however, attributed the development of CCl_4-induced liver fibrosis to STING-mediated activation of hepatocellular death pathways. This appeared to not have human relevance because STING is not present in human hepatocytes. We argue that the STING found in cells other than hepatocytes appears to trigger or exacerbate liver fibrotic program. Indeed, we validated that STING activation directly activates HSCs evidenced by the finding that treatment with DMXAA caused significant increases in TGFβ1-stimulated phosphorylation states of p38 and amount of αSMA in LX2 cells. This suggests the involvement of the STING in HSCs in MCD-induced liver fibrosis, unlike in CCl_4-induced model where CCl_4 did not alter STING signaling in HSCs. More importantly, we further validated that the STING in macrophages acted through a paracrine manner to regulate HSC activation. As supporting evidence, treatment of LX2 cells with conditioned media of DMXAA-treated WT macrophages, but not conditioned media of DMXAA-treated STING^{gt} macrophages, significantly increased p38 phosphorylation, αSMA amount, and the mRNA levels of αSMA, Col1a1, and Fn, which are indicative of HSC activation. At this point, it is not clear of the proportional contributions of the STING in HSC vs. macrophages in regulating HSC activation. Considering that livers of MCD-fed WT mice contained massive aggregations of macrophages/Kupffer cells, we argue a more important role for the STING in macrophages in pathogenesis of liver fibrosis through paracrine mechanisms to activate HSCs.

STING disruption also decreased HFD-induced insulin resistance, which contributes to NAFLD pathogenesis. To date, there is no available evidence indicating direct interactions between STING and the components of insulin signaling pathway. While addressing the effects of disrupting STING (in endothelial cells) and/or signaling molecules downstream of STING on regulating systemic insulin sensitivity [29, 34, 35], limited studies have suggested that STING-TBK1-IRF3 pathway(s) act through inflammatory mechanisms to impair insulin signaling. Given this, STING disruption likely acts through suppressing inflammation to improve insulin sensitivity.

In summary, we established a link between STING and NAFLD/NASH in both mouse models and human patients' samples. Specifically, we showed increased liver signaling events downstream of STING in a mouse model of NAFLD, and revealed, for the first time, that STING expression is increased in hepatic non-parenchymal cells of human patients with NAFLD. We further demonstrated that STING plays a deleterious role in NAFLD/NASH and this role was achieved through enhancing macrophage proinflammatory activation. Therefore, targeting STING to inhibiting macrophage proinflammatory activation is a viable therapeutic or preventive approach for the management of NAFLD/NASH.

Supplementary Material

Refer to Web version on PubMed Central for supplementary material.

Acknowledgments

FUNDING

This work was supported in whole or in part by grants from the American Diabetes Association (1–17-IBS-145) and the National Institutes of Health (DK095862) to C.W. This work was also supported in part by the Dr. Nicholas C. Hightower Centennial Chair of Gastroenterology from Scott & White, a VA Research Career Scientist Award to G.A. and the NIH grants DK076898, DK110035, DK062975, AA025157, AA025997, and DK054811 to G.A, F.M. and S.G, and by a VA Merit Award (1I01BX003031) and an NIH grant (DK108959) to H.F. Also, C.W. is supported by the Hatch Program of the National Institutes of Food and Agriculture (NIFA).

Abbreviations

ACC1	acetyl-CoA carboxylase 1
ALD	alcoholic fatty liver disease
αSMA	α-smooth muscle actin
BMDM	bone marrow-derived macrophages
BSA	bovine serum albumin
CD	chow diet
Col1a1	collagen Type I alpha 1
CPT1a	carnitine palmitoyltransferase1a
DMEM	Dulbecco's modified Eagle's medium

DMXAA	5,6-dimethylxanthenone-4-acetic acid
FAS	fatty acid synthase
FBS	fetal bovine serum
FFA	free fatty acids
FN	fibronectin
GAPDH	glyceraldehyde 3-phosphate dehydrogenase
GTT	glucose tolerance test
H&E	hematoxylin and eosin
HFD	high-fat diet
HSCs	hepatic stellate cells
LFD	low-fat diet
IFNβ	interferon beta
IL-1β	interleukin 1β
IL-4	interleukin 4
IL-6	interleukin 6
IMDM	Iscove's Modified Dulbecco's medium
ITT	insulin tolerance test
LPS	lipopolysaccharide
IRF3	interferon regulatory factor 3
JNK	c-Jun N-terminal kinases
MCD	methionine- and choline-deficient diet
MMP2	matrix metallopeptidase 2
NAFLD	non-alcoholic fatty liver disease
NFκB	nuclear factor kappa B
NASH	non-alcoholic steatohepatitis
Pp65	phosphorylated p65 subunit of NFκB
Pp46	phosphorylated JNK1 (p46)
PPARγ	peroxisome proliferator-activated receptor gamma
RQ	respiratory quotient

SREBP1c	sterol regulatory element-binding protein 1c
STING	stimulator of interferon genes
TBK1	TANK-binding kinase 1
TG	triglycerides
TNFα	tumor necrosis factor α
TGFβ1	transforming growth factor β1

REFERENCES

1. Sanyal AJ. Mechanisms of Disease: pathogenesis of nonalcoholic fatty liver disease. Nat Clin Pract Gastroenterol Hepatol 2005;2:46–53. [PubMed: 16265100]
2. Chalasani N, Younossi Z, Lavine JE, et al. The diagnosis and management of nonalcoholic fatty liver disease: Practice guidance from the American Association for the Study of Liver Diseases. Hepatology 2018;67:328–357. [PubMed: 28714183]
3. Farrell GC, Larter CZ. Nonalcoholic fatty liver disease: From steatosis to cirrhosis. Hepatology 2006;43:S99–S112. [PubMed: 16447287]
4. Younossi ZM, Koenig AB, Abdelatif D, et al. Global epidemiology of nonalcoholic fatty liver disease-Meta-analytic assessment of prevalence, incidence, and outcomes. Hepatology 2016;64:73–84. [PubMed: 26707365]
5. Estes C, Razavi H, Loomba R, et al. Modeling the epidemic of nonalcoholic fatty liver disease demonstrates an exponential increase in burden of disease. Hepatology (Baltimore, Md.) 2018;67:123–133.
6. Caldwell SH, Crespo DM, Kang HS, et al. Obesity and hepatocellular carcinoma. Gastroenterology 2004;127:S97–S103. [PubMed: 15508109]
7. Powell EE, Jonsson JR, Clouston AD. Steatosis: Co-factor in other liver diseases. Hepatology 2005;42:5–13. [PubMed: 15962320]
8. Starley BQ, Calcagno CJ, Harrison SA. Nonalcoholic fatty liver disease and hepatocellular carcinoma: a weighty connection. Hepatology 2010;51:1820–1832. [PubMed: 20432259]
9. Younossi ZM, Otgonsuren M, Henry L, et al. Association of nonalcoholic fatty liver disease (NAFLD) with hepatocellular carcinoma (HCC) in the United States from 2004 to 2009. Hepatology 2015;62:1723–1730. [PubMed: 26274335]
10. Angulo P NAFLD, Obesity, and Bariatric Surgery. Gastroenterology 2006;130:1848–1852. [PubMed: 16697746]
11. Neuschwander-Tetri BA. NASH: Thiazolidinediones for NASH--one pill doesn't fix everything. Nat Rev Gastroenterol Hepatol 2010;7:243–244. [PubMed: 20442730]
12. Deng Z, Liu Y, Cunren Liu C, et al. Immature myeloid cells induced by a high-fat diet contribute to liver inflammation. Hepatology 2009;50:1412–1420. [PubMed: 19708080]
13. Huang W, Metlakunta A, Dedousis N, et al. Depletion of liver Kupffer cells prevents the development of diet-induced hepatic steatosis and insulin resistance. Diabetes 2010;59:347–357. [PubMed: 19934001]
14. Xu H, Li H, Woo S-L, et al. Myeloid cell-specific disruption of Period1 and Period2 exacerbates diet-induced inflammation and insulin resistance. J Biol Chem 2014;289:16374–16388. [PubMed: 24770415]
15. Cai Y, Li H, Liu M, et al. Disruption of adenosine 2A receptor exacerbates NAFLD through increasing inflammatory responses and SREBP1c activity. Hepatology 2018;68:48–61. [PubMed: 29315766]
16. Kodama Y, Kisseleva T, Iwaisako K, et al. c-Jun N-terminal kinase-1 from hematopoietic cells mediates progression from hepatic steatosis to steatohepatitis and fibrosis in mice. Gastroenterology 2009;137:1467–1477.e5. [PubMed: 19549522]

17. Ishikawa H, Barber GN. STING an endoplasmic reticulum adaptor that facilitates innate immune signaling. Nature 2008;455:674–678. [PubMed: 18724357]
18. Sun L, Wu J, Du F, et al. Cyclic GMP-AMP synthase is a cytosolic DNA sensor that activates the type I interferon pathway. Science 2013;339:786–791. [PubMed: 23258413]
19. Petrasek J, Iracheta-Vellve A, Csak T, et al. STING-IRF3 pathway links endoplasmic reticulum stress with hepatocyte apoptosis in early alcoholic liver disease. Proceedings of the National Academy of Sciences of the United States of America 2013;110:16544–16549. [PubMed: 24052526]
20. Deng L, Liang H, Xu M, et al. STING-dependent cytosolic DNA sensing promotes radiation-induced type I interferon-dependent antitumor immunity in immunogenic tumors. Immunity 2014;41:843–852. [PubMed: 25517616]
21. Paijo J, Döring M, Spanier J, et al. cGAS sense s human cytomegalovirus and induces type I interferon responses in human monocyte-derived cells. PLoS Pathog 2016;12:e1005546. [PubMed: 27058035]
22. Thomsen MK, Nandakumar R, Stadler D, et al. Lack of immunological DNA sensing in hepatocytes facilitates hepatitis B virus infection. Hepatology 2016;64:746–759. [PubMed: 27312012]
23. Iracheta-Vellve A, Petrasek J, Gyongyosi B, et al. Endoplasmic reticulum stress-induced hepatocellular death pathways mediate liver injury and fibrosis via stimulator of interferon genes. J Biol Chem 2016;291:26794–26805. [PubMed: 27810900]
24. Cho C-S, Park H-W, Ho A, et al. Lipotoxicity induces hepatic protein inclusions through TBK1-mediated p62/SQSTM1 phosphorylation. Hepatology 2017:n/a-n/a.
25. Qiao JT, Cui C, Qing L, et al. Activation of the STING-IRF3 pathway promotes hepatocyte inflammation, apoptosis and induces metabolic disorders in nonalcoholic fatty liver disease. Metabolism 2018;81:13–24. [PubMed: 29106945]
26. Guo X, Shu C, Li H, et al. Cyclic GMP-AMP ameliorates diet-induced metabolic dysregulation and regulates proinflammatory responses distinctly from STING activation. Sci Rep 2017;7:6355. [PubMed: 28743914]
27. Conlon J, Burdette DL, Sharma S, et al. Mouse, but not human STING, binds and signals in response to the vascular disrupting agent 5,6-dimethylxanthenone-4-acetic acid. J Immunol 2013;190:5216–5225. [PubMed: 23585680]
28. Liu S, Cai X, Wu J, et al. Phosphorylation of innate immune adaptor proteins MAVS, STING, and TRIF induces IRF3 activation. Science 2015;347.
29. Mao Y, Luo W, Zhang L, et al. STING-IRF3 triggers endothelial inflammation in response to free fatty acid-induced mitochondrial damage in diet-induced obesity. Arterioscler Thromb Vasc Biol 2017;37:920–929. [PubMed: 28302626]
30. Tian L, Changzheng L, Guizhi Y, et al. Sphingosine kinase 1 promotes liver fibrosis by preventing miR-19b-3p-mediated inhibition of CCR2. Hepatology 2018;0.
31. Larkin B, Ilyukha V, Sorokin M, et al. Cutting Edge: Activation of STING in T cells induces Type I IFN responses and cell death. J Immunol 2017;199:397. [PubMed: 28615418]
32. Gandhi CR, Chaillet JR, Nalesnik MA, et al. Liver-specific deletion of augmenter of liver regeneration accelerates development of steatohepatitis and hepatocellular carcinoma in mice. Gastroenterology 2015;148:379–391.e4. [PubMed: 25448926]
33. Schuster S, Cabrera D, Arrese M, et al. Triggering and resolution of inflammation in NASH. Nat Rev Gastroenterol Hepatol 2018;15:349–364. [PubMed: 29740166]
34. Kumari M, Wang X, Lantier L, et al. IRF3 promotes adipose inflammation and insulin resistance and represses browning. J Clin Invest 2016;126:2839–2854. [PubMed: 27400129]
35. Zhao P, Wong Ki, Sun X, et al. TBK1 at the Crossroads of Inflammation and Energy Homeostasis in Adipose Tissue. Cell 2018;172:731–743.e12. [PubMed: 29425491]

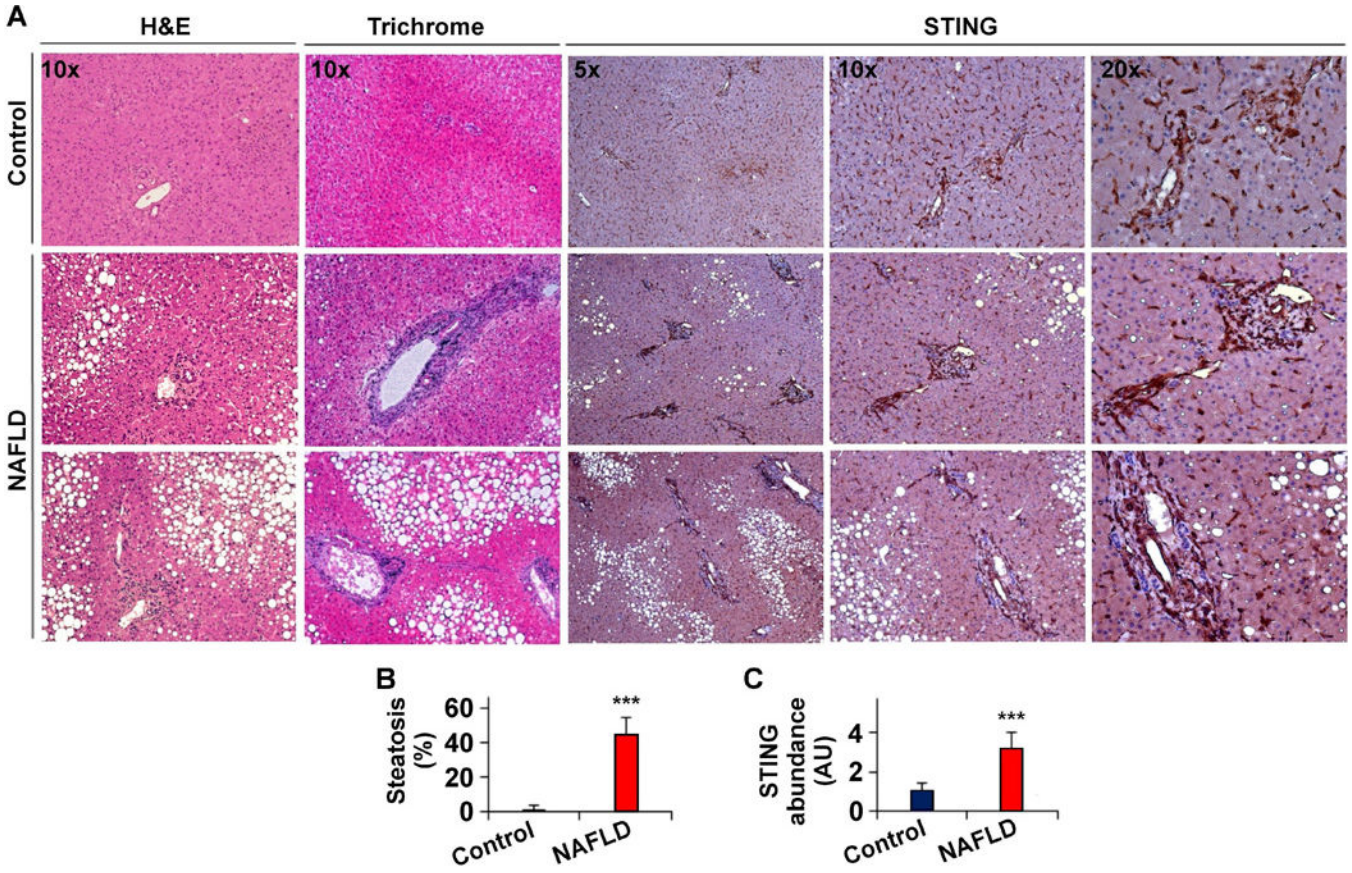

Figure 1. STING expression is increased in livers of human patients with NAFLD

(**A**) Liver sections of NAFLD patients (bottom two rows) and human subjects without NAFLD (Control, top row) were stained with H&E (the very left column) and Trichrome (the second left column), and examined for STING expression (the right three columns). (**B**) Degrees of hepatic steatosis. (**C**) STING abundance in liver sections. AU, arbitrary unit. For bar graphs, data are means ± SD. n = 6 – 8. ***, $P < 0.001$ NAFLD vs. Control.

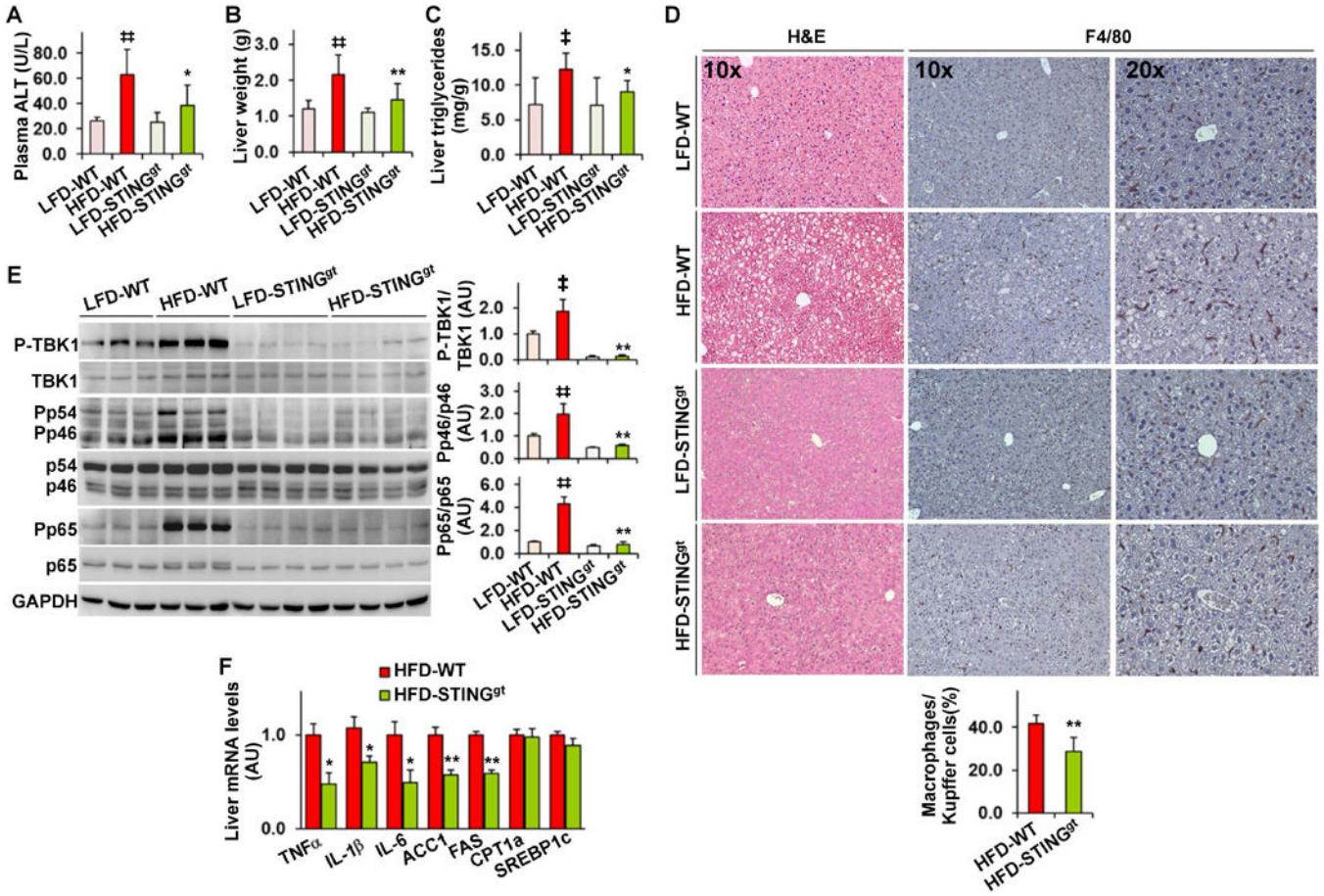

Figure 2. STING disruption protects against HFD-induced NAFLD

Male STING-disrupted (STING^{gt}) mice and WT mice, at 5 – 6 weeks of age, were fed an LFD or HFD for 12 weeks. (**A**) Plasma levels of alanine aminotransferase (ALT). (**B**) Liver weight. (**C**) Liver levels of triglycerides. (**D**) Liver sections were stained with H&E (left column) or for F4/80 expression (right two columns). Bar graph, percentages of macrophages. (**E**) Liver lysates were examined for inflammatory signaling using Western blot analysis. Bar graphs, quantification of blots. (**F**) Liver mRNA levels were examined using real-time RT-PCR. For all bar graphs, data are means ± SD. n = 10 – 12. ‡, $P < 0.05$ and ‡‡, $P < 0.01$ HFD-WT vs. LFD-WT in A - C, and E; *, $P < 0.05$ and **, $P < 0.01$ HFD-STING^{gt} vs. HFD-WT (in A - E) for the same gene (in F).

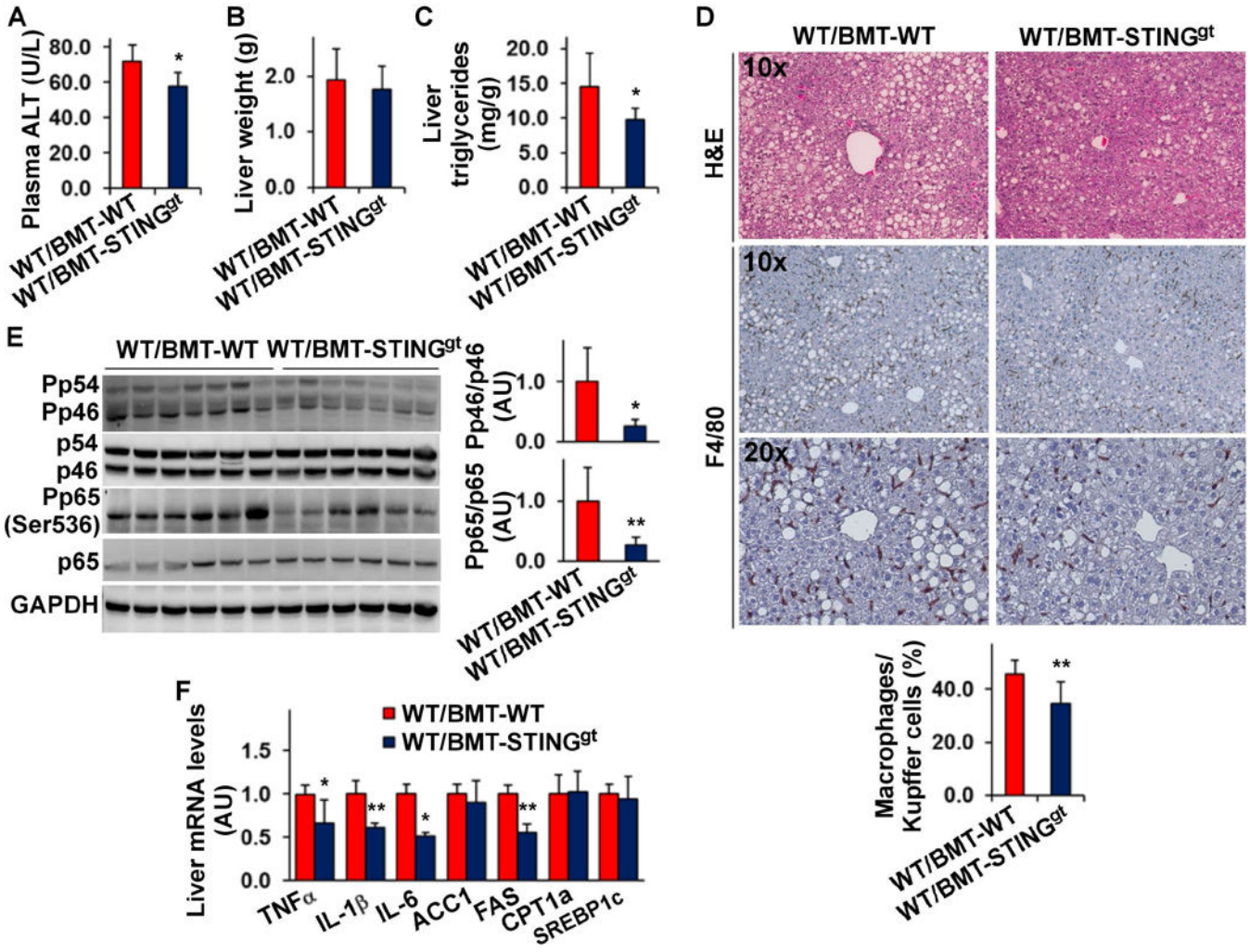

Figure 3. Myeloid cell-specific STING disruption decreases the severity of HFD-induced NAFLD

Male WT C57BL/6J mice, at 5 – 6 weeks of age, were lethally irradiated and transplanted with bone marrow cells from STING^{gt} and/or WT mice. After recovery for 4 weeks, the chimeric mice were fed an HFD for 12 weeks. (**A**) Plasma levels of ALT. (**B**) Liver weight. (**C**) Liver levels of triglycerides. (**D**) Liver sections were stained with H&E (top row) or for F4/80 expression (bottom two rows). Bar graph, percentages of macrophages. (**E**) Liver lysates were examined for proinflammatory signaling using Western blot analysis. Bar graphs, quantification of blots. (**F**) Liver mRNA levels were examined using real-time RT-PCR. For A - F, WT/BMT-STING^{gt}, WT mice received STING^{gt} bone marrow cells; WT/BMT-WT, WT mice received WT bone marrow cells. For all bar graphs, data are means ± SD. n = 8 – 10. *, $P < 0.05$ and **, $P < 0.01$ WT/BMT-STING^{gt} vs. WT/BMT-WT (in A, and C- E) for the same gene (in F).

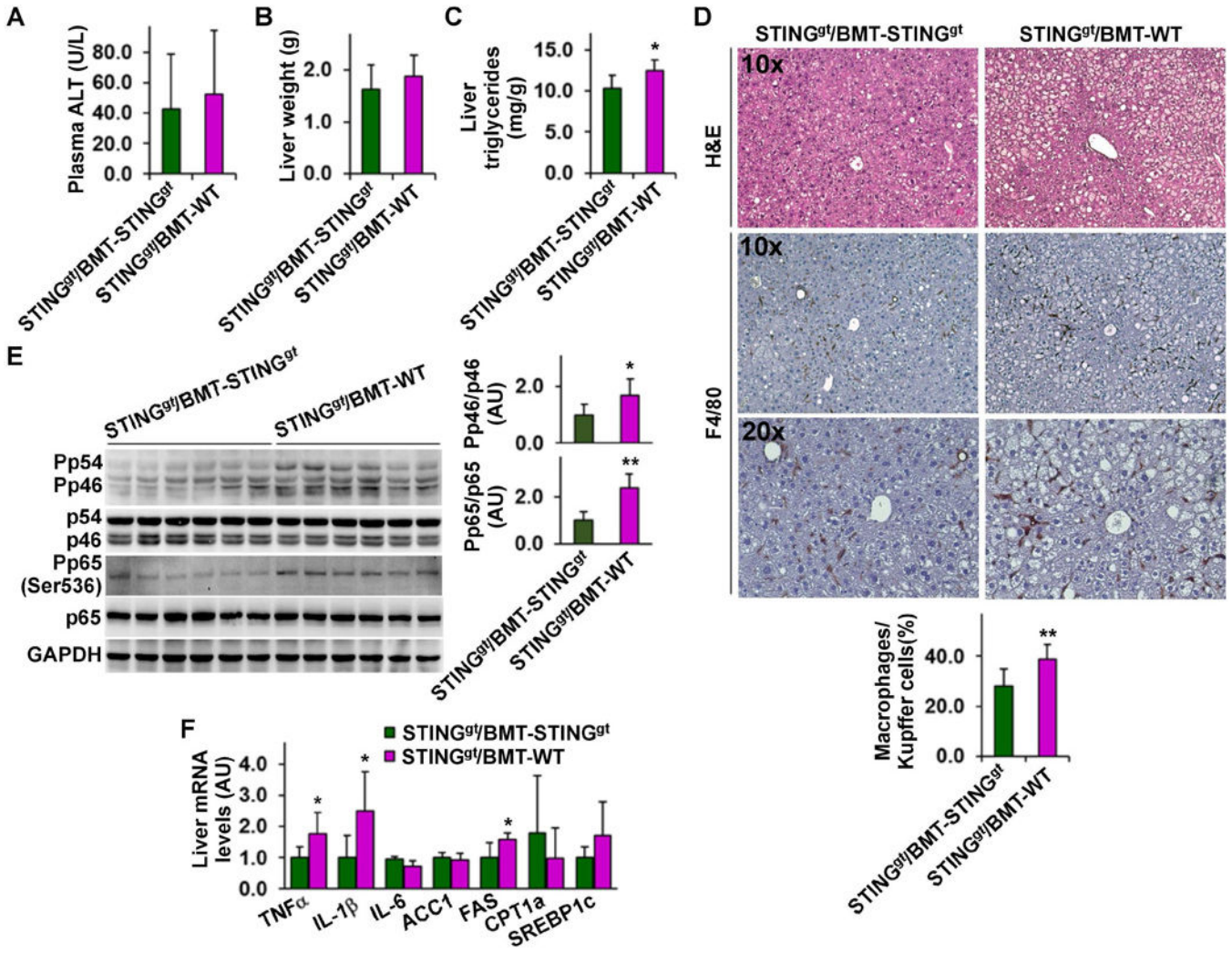

Figure 4. STING presence only in myeloid cells exacerbates HFD-induced NAFLD

Male STING^{gt} mice, at 5 – 6 weeks of age, were lethally irradiated and transplanted with bone marrow cells from WT and/or STING^{gt} mice. After recovery for 4 weeks, the chimeric mice were fed an HFD for 12 weeks. (**A**) Plasma levels of ALT. (**B**) Liver weight. (**C**) Liver levels of triglycerides. (**D**) Liver sections were stained with H&E (top row) or for F4/80 expression (bottom two rows). Bar graph, percentages of macrophages. (**E**) Liver lysates were examined for proinflammatory signaling using Western blot analysis. Bar graphs, quantification of blots. (**F**) Liver mRNA levels were examined using real-time RT-PCR. For A - F, STING^{gt}/BMT-WT, STING^{gt} mice received WT bone marrow cells; STING^{gt}/BMT-STING^{gt}, STING^{gt} mice received STING^{gt} bone marrow cells. For all bar graphs, data are means ± SD. n = 10 – 12. *, $P < 0.05$ and **, $P < 0.01$ STING^{gt}/BMT-WT vs. STING^{gt}/BMT-STING^{gt} (in C - E) for the same gene (in F).

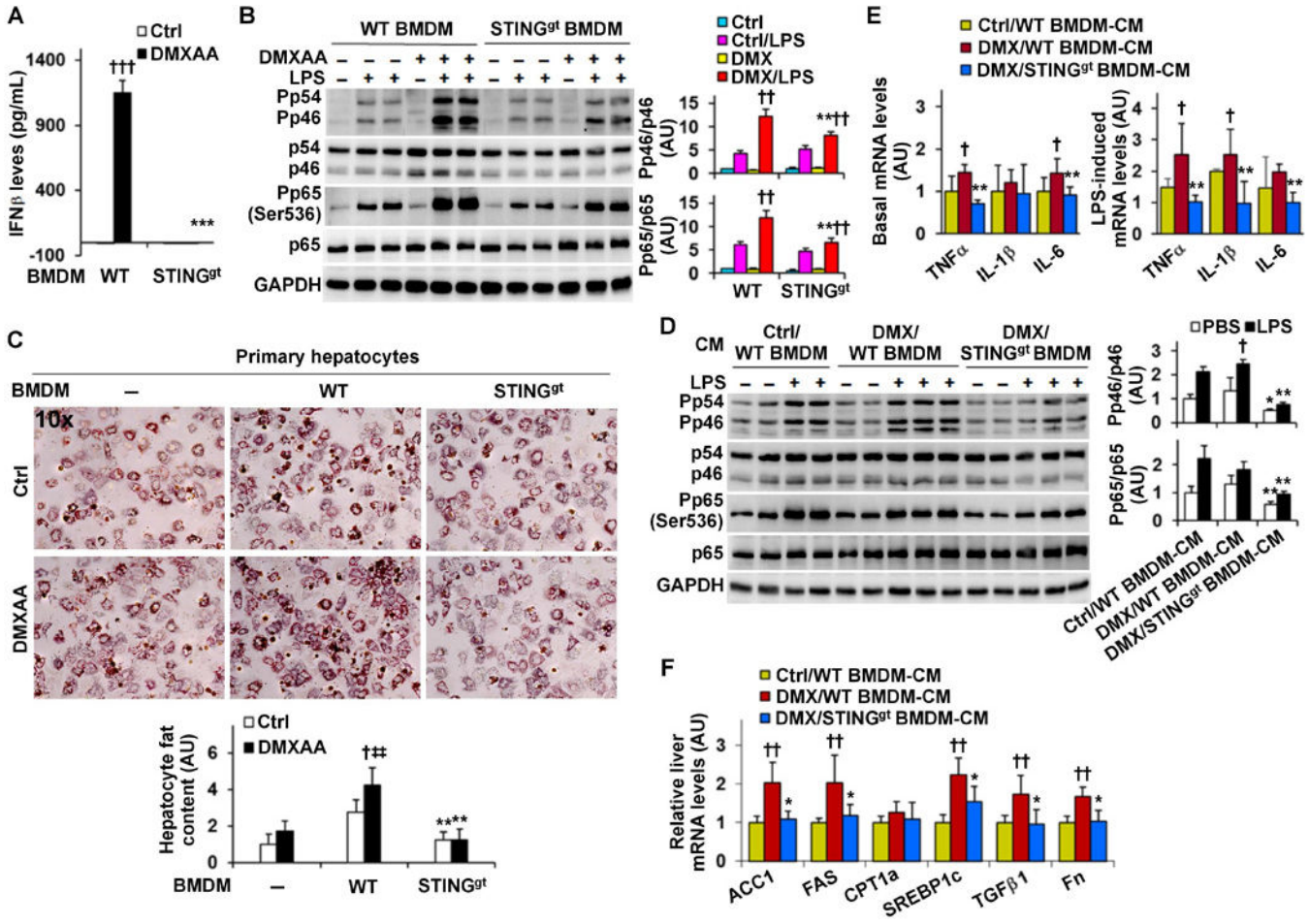

Figure 5. STING enables macrophages to generate factors that promote hepatocyte fat deposition and proinflammatory responses

Macrophages and primary hepatocyte were prepared from male STING^{gt} mice and WT C57BL/6J mice as described in Methods. (**A**) Macrophage interferon beta (IFNβ) production. Bone marrow-derived macrophages (BMDM) were treated with DMXAA (75 μg/mL) or control (Ctrl, 7.5% NaHCO3) for 6 hr. BMDM-conditioned media were examined for IFNβ levels. (**B**) Macrophage proinflammatory signaling. BMDM were treated with or without DMXAA (75 μg/mL) for 24 hr in the absence or presence of LPS (100 ng/mL) for the last 30 min. (**C**) Hepatocyte fat deposition of co-cultures. Primary hepatocytes were incubated in the absence of macrophages or co-cultured with BMDM from WT or STING^{gt} mice for 48 hr, and treated with DMXAA (75 μg/mL) or control in the presence of palm itate (250 μM) for the last 24 hr. Prior to harvest, hepatocytes or co-cultures were stained with oil red O for 1 hr. Bar graph, quantification of fat content. (**D**, **E**, **F**) Macrophage factors regulation of hepatocyte proinflammatory responses and gene expression. Conditioned media (CM) were collected from DMXAA (DMX)-treated WT BMDM, DMX-treated STING^{gt} BMDM, and Ctrl-treated WT BMDM (described in B) and designated as DMX/WT BMDM-CM, DMX/STING^{gt} BMDM-CM, and Ctrl/WT BMDM-CM, respectively. CM were mixed with fresh media at a 1:1 ratio and supplemented to hepatocytes for 48 hr. Prior to harvest, CM-incubated hepatocytes were treated with or

without LPS (100 ng/mL) for 30 min (D) or LPS (20 ng/mL) for 6 hr (E). For B and D, cell lysates were examined for proinflammatory signaling using Western blot analysis. Bar graphs, quantification of blots. For E and F, the mRNA levels were examined using real-time RT-PCR. For bar graphs in A - F, data are means ± SD. n = 6 – 8 (A, E, and F) or 4 – 6 (B, C, and D). *, $P < 0.05$, **, $P < 0.01$, and ***, $P < 0.001$ $STING^{gt}$ vs. WT with the same treatment (Ctrl or DMXAA in A and C; Ctrl/LPS or DMX/LPS in B) or DMX/$STING^{gt}$ BMDM-CM vs. DMX/WT BMDM-CM under the same condition (PBS or LPS in D) or for the same gene (in E and F); †, $P < 0.05$, ††, $P < 0.01$, and †††, $P < 0.001$ DMXAA vs. Ctrl (in A and C) or DMX/LPS vs. Ctrl/LPS (in B) within the same genotype, or DMX/WT BMDM-CM vs. Ctrl/WT BMDM-CM under LPS-stimulated condition (in D) or for the same gene (in E and F); ‡‡, $P < 0.01$ hepatocytes co-cultured with WT BMDM vs. hepatocytes alone in the presence of DMXAA (in C).

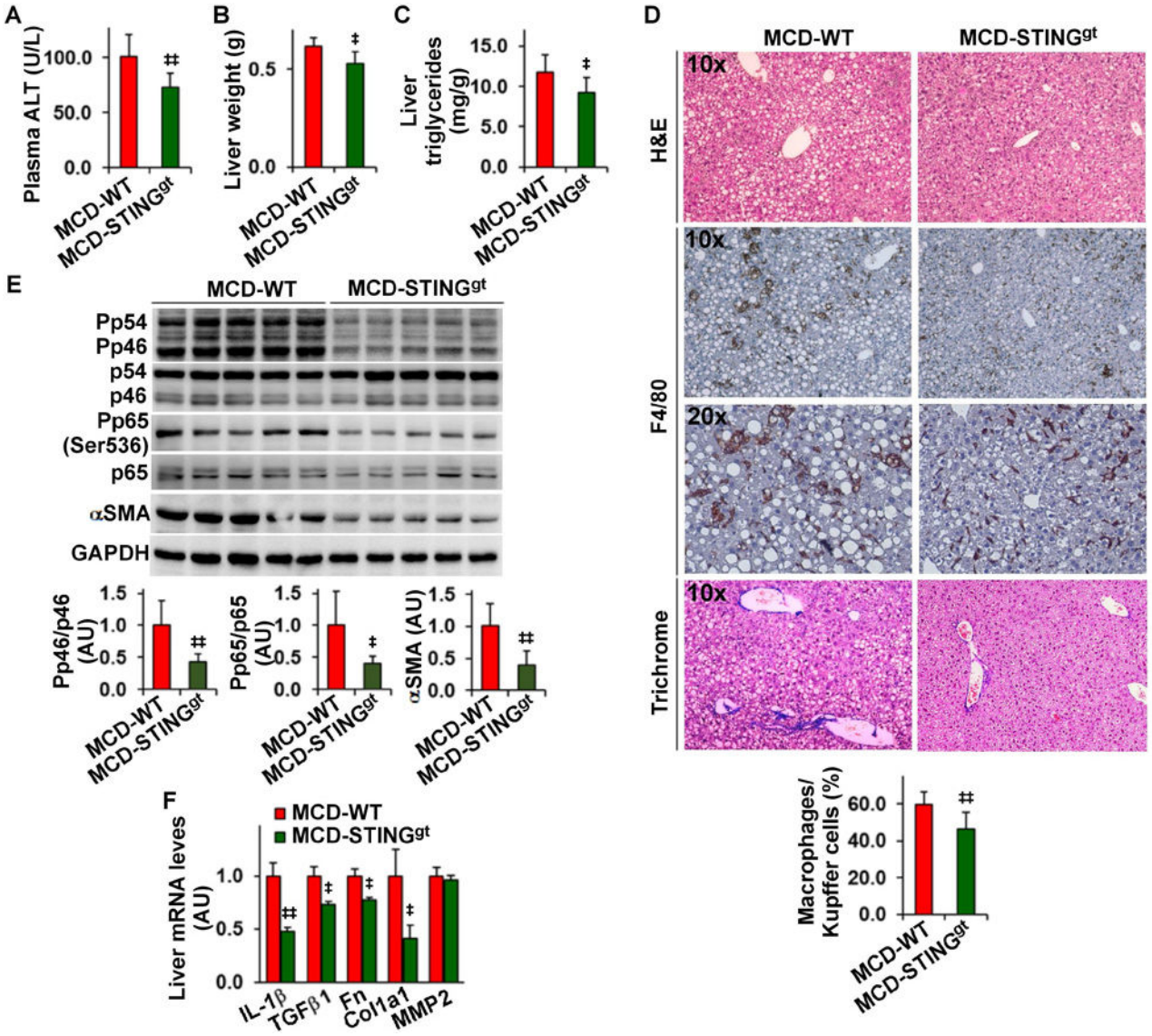

Figure 6. STING disruption decreases the severity of MCD-induced NASH

Male STING^{gt} mice and WT C57BL/6J mice, at 11 – 12 weeks of age, were fed an MCD for 5 weeks. (**A**) Plasma levels of ALT. (**B**) Liver weight. (**C**) Liver levels of triglycerides. (**D**) Liver sections were stained with H&E (top row), for F4/80 expression (middle two rows), or with Trichrome (bottom row). Bar graph, percentages of macrophages. (**E**) Liver lysates were examined for inflammatory signaling and αSMA amount using Western blot analysis. Bar graphs, quantification of blots. (**F**) Hepatic expression of genes related to fibrosis was examined using real-time RT-PCR. MMP2, matrix metalloproteinase 2. For bar graphs in A - F, data are means ± SD. n = 8 – 10 (A - D) or 6 – 8 (E and F)., $P < 0.05$ and, $P < 0.01$ MCD-STING^{gt} vs MCD-WT (in A - E) for the same gene (in F).

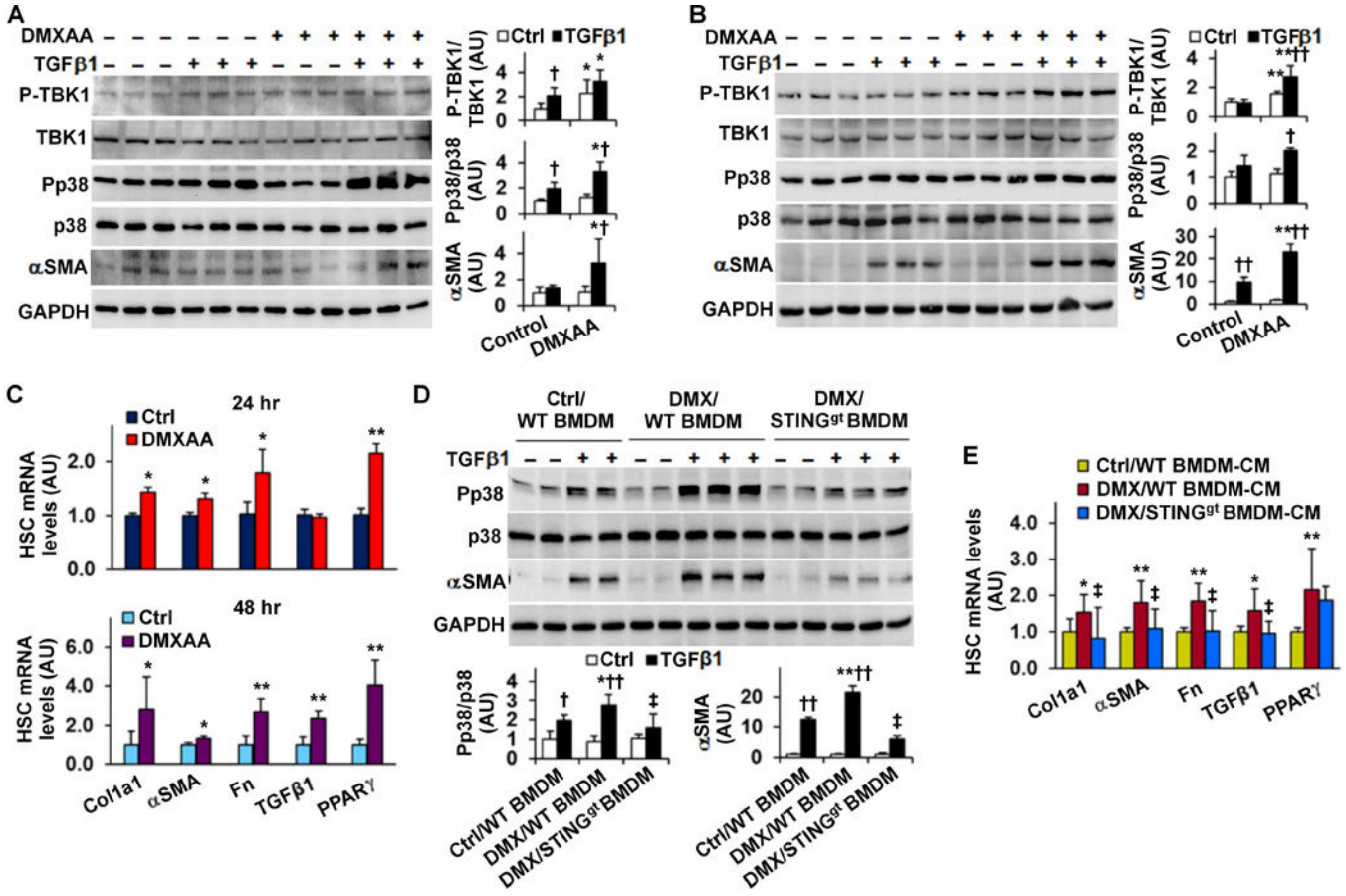

Figure 7. STING increases HSC activation status and enables macrophage factors to enhance HSC activation (A, B, C)

Activating STING enhances HSC activation. For A - C, LX2 cells were treated with or without DMXAA (75 μg/mL) in the absence or presence of TGFβ1 (8 ng/mL) for 24 hr (A and C (top panel)) or TGFβ1 (2.5 ng/mL) for 48 hr (B and C (bottom panel)). (**D**, **E**) STING-driven macrophage factors enhance HSC activation. For D, LX2 cells were co-cultured with STING^{gt} BMDM and/or WT BMDM that were pre-treated with DMXAA (75 μg/mL) or Ctrl for 24 hr. The co-cultures were incubated for 48 hr in the absence or presence of TGFβ1 (2.5 ng/mL). For E, LX2 cells were treated with conditioned media (CM) of DMXAA (DMX)- or Ctrl-treated WT BMDM and/or STING^{gt} BMDM for 48 hr. For A, B, and D, cell lysates were subjected to Western blot analysis. Bar graphs, quantification of blots. For C and E, the expression of fibrogenic genes was examined using real-time RT-PCR. For bar graphs in A - E, data are means SD. n = 4 – 6 (A, B, and D) or 6 – 8 (C and E). *, $P < 0.05$ and **, $P < 0.01$ DMXAA vs. Control (Ctrl) under the same condition (in A and B) or for the same gene (in C), co-cultures with DMX/WT BMDM vs. co-cultures with Ctrl/WT BMDM under the same condition (in D), or DMX/WT BMDM-CM-treated HSCs vs. Ctrl/WT BMDM-CM-treated HSCs for the same gene (in E); †, $P < 0.05$ and ††, $P < 0.01$ TGFβ1 vs. Ctrl with the same treatment (in A, B, and D); ‡, $P < 0.05$ DMX/STING^{gt} BMDM-CM-treated HSCs vs. DMX/WT BMDM-CM-treated HSCs under TGFβ1-stimulated condition (in D) or for the same gene (in E).